Inclusion compounds with mixed guests: controlled stoichiometries and kinetics of enclathration

Leonard J. Barbour,[a] Mino R. Caira,[b] Tanya le Roex[b] and Luigi R. Nassimbeni*[b]

[a] *Department of Chemistry, University of Missouri-Columbia, Columbia, Missouri 65211, USA*
[b] *Department of Chemistry, University of Cape Town, Rondebosch 7701, South Africa. E-mail: xrayluig@science.uct.ac.za*

Received (in Cambridge, UK) 30th November 2001, Accepted 3rd October 2002
First published as an Advance Article on the web 1st November 2002

The host compound *trans*-9,10-dihydroxy-9,10-bis(*p-tert*-butylphenyl)-9,10-dihydroanthracene forms inclusion compounds with DMF, DMSO and acetone of the type $H{\cdot}nG_1{\cdot}(4-n)G_2$, with n varying integrally from 0 to 4. The structures of these compounds have been elucidated. The kinetics of enclathration with acetone vapour displays anti-Arrhenius behaviour and the desorption process has a low activation energy of 48.4 kJ mol^{-1}.

Introduction

Inclusion compounds containing more than one kind of guest molecule are well established in the literature. They often arise from the use of solvent mixtures in the crystallisation of the desired compound. A survey giving a statistical analysis of the inclusion of solvent molecules in the crystal structures of organic and metalloorganic compounds has appeared recently.[1] Here it is pointed out that water is the most common molecule occurring as a co-solvate, and there are several examples of inclusion compounds which contain three or four different guest molecules and the structure of zinc(II)tetrakis(pentafluorophenyl)-β-octabromoporphyrin incorporates no fewer than five different solvents: carbon tetrachloride, *o*-dichlorobenzene, acetone, methanol and water.[2]

There are a number of papers which deal specifically with the properties of inclusion compounds containing more than one guest: bulky hosts containing the fluorenyl moiety have been shown to enclathrate n-propanol, and the resulting inclusion compound, upon exposure to i-propanol, allows guest exchange, yielding a final 1:1:1 ternary clathrate.[3]

The effect of several solvents on the inclusion of 2-acetylnaphthalene in the host 1,1-di(4-hydroxyphenyl)cyclohexane has been investigated and the thermal behaviour of the resulting solid solutions has been measured by DSC.[4]

Several organic host compounds have been studied extensively and their selectivity has been established *via* competition experiments between similar guests. In general, three kinds of selectivity curves arise, as shown in Fig. 1.

X_B is the mole fraction of guest B in the liquid mixture and Z_B that of guest B which has been enclathrated in the host–guest crystal. The broken diagonal line represents zero selectivity. Curve *a* represents poor selectivity and is likely to arise when the pure compounds $H{\cdot}A_n$ and $H{\cdot}B_n$ are isostructural with respect to the host structure and the guests A and B are located in similar positions of the host lattice, thus facilitating guest exchange. An example of this occurs with the host 1,4-bis(9-hydroxyfluorenyl-9-yl)benzene, which forms inclusion compounds with acetone and DMSO and the guests are readily exchanged.[5]

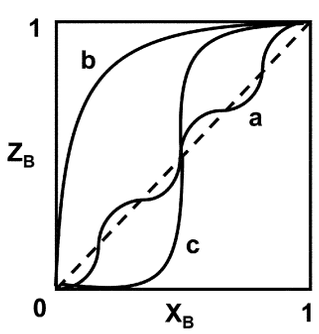

Fig. 1 Typical selectivity curves obtained from competition experiments.

Curve *b* occurs when guest B is strongly selected over guest A for the whole concentration range. From the practical aspect of efficient separation, this is the more desirable result. This has been demonstrated in the separation of isomeric mixtures of xylenes and dimethylnaphthalenes by guanidium organodisulfonate hosts[6] and in the selective inclusion of aliphatic alcohols by 1,1-bis(4-hydroxyphenyl)cyclohexane, in which the competition was carried out with four different alcohols simultaneously.[7]

Curve *c* occurs when the selectivity is concentration dependent, as occurs in the separation of 2,4-lutidine and 2,6-lutidine by 2,2′-dihydroxy-1,1′-binaphthyl.[8] An important aspect of this kind of selectivity occurs in the separation of 3- and 4-picolines by bulky diol hosts.[9] In this study it was shown that the selectivity curve changed position depending on the presence of neutral solvents, but no systematic work on this aspect was carried out.

In this work, however, we present results of a host–guest system which behaves in a totally different manner. The host *trans*-9,10-dihydroxy-9,10-bis(*p-tert*-butylphenyl)-9,10-dihydroanthracene, H, forms inclusion compounds with *N*,*N*-dimethylformamide, A, and dimethylsulfoxide, B, and yields compounds of the type $H{\cdot}nA{\cdot}(4-n)B$, with n varying integrally from 0 to 4.

We have also elucidated the structure of the α, non-porous phase of the apohost, its inclusion compound with acetone, H·4C and the ternary compounds H·2A·2C and H·2B·2C. In addition we have studied the kinetics of enclathration of the host with acetone vapour and the kinetics of desorption of the acetone inclusion compound.

Results and discussion

The structural formula of the host, with its atomic nomenclature, and that of the various guests, is shown in Scheme 1. The results of the DMF–DMSO competition experiments are

DOI: 10.1039/b110987c

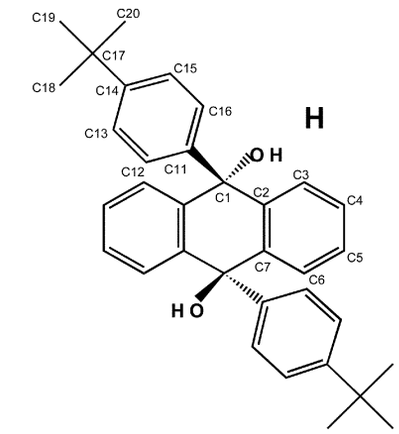

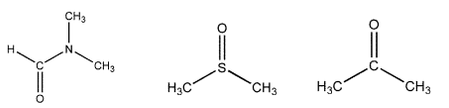

A = DMF **B** = DMSO **C** = acetone

1 = H (apohost) **4** = H·2A·2B **7** = H·4C
2 = H·4A **5** = H·A·3B **8** = H·2A·2C
3 = H·3A·B **6** = H·4B **9** = H·2B·2C

Scheme 1

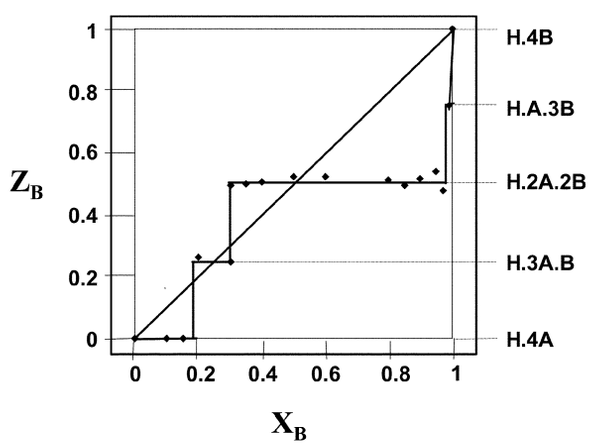

Fig. 2 Results of the DMF–DMSO competition experiments. Figure reproduced from ref. 10 by permission of The Royal Society of Chemistry.

shown in Fig. 2, which reveals that the stoichiometry of the inclusion compounds varies in discrete steps, giving rise to five distinct compounds: H·4A, H·3A·B, H·2A·2B, H·A·3B and H·4B. The stoichiometry is controlled by changing the composition of the liquid guest mixture, and a preliminary communication of this result has appeared.[10]

The TG and DSC curves for H·2A·2B are shown in Fig. 3. This shows that the compound desolvates in two distinct steps, the first due to the loss of two DMF molecules and the second due to the two DMSO molecules. The DSC shows the corresponding endotherms followed by a third peak due to the melting of the host. Similar curves were obtained for all the remaining inclusion compounds with DMF, DMSO and acetone, allowing us to establish the stoichiometry of each compound unambiguously.

The compound H·A·3B was difficult to isolate because when the liquid guest is in the mole fraction range $X_B = 0.5$–1.0 the host shows a strong propensity for the formation of H·2A·2B. We therefore prepared H·A·3B by using an initial mixture with a mole fraction $X_B = 0.99$.

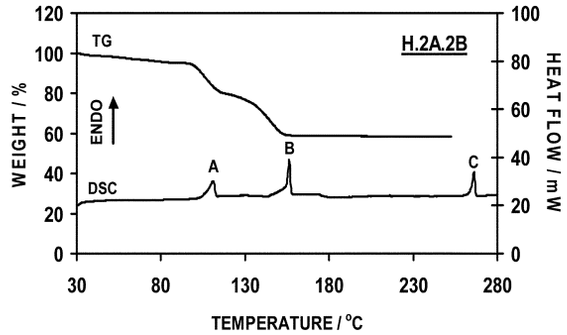

Fig. 3 TG and DSC curves for H·2A·2B. Figure reproduced from ref. 10 by permission of The Royal Society of Chemistry.

The crystal and experimental data are given in Table 1.† The structure of the non-porous, α-phase, the apohost, is shown in Fig. 4. This structure is monoclinic and crystallises in the space

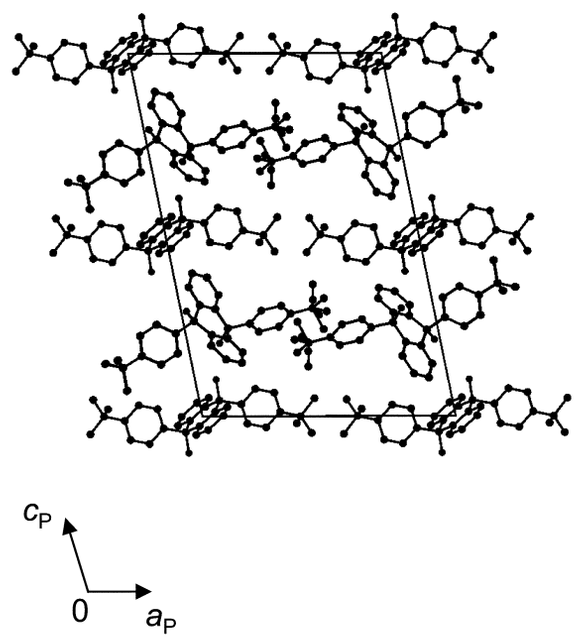

Fig. 4 Projection of the apohost structure along [010].

group $P2_1/c$, with six molecules per unit cell. The asymmetric unit consists of one complete host molecule and one half of a host molecule. In the unit cell, four host molecules lie in general positions and two molecules lie on centres of inversion in positions 0,1/2,0 and 0,0,1/2 (Wyckoff position c).

The molecules pack to form planes perpendicular to [100]. Within these planes there is a circular pattern of hydrogen bonds which interlink eight host molecules. Host molecule A, which lies on a centre of inversion, is stabilised by a (Host A)–O1–H1 ··· O21(Host B^1) hydrogen bond (d(O ··· O) = 2.816(2) Å). Host B^1 in turn hydrogen bonds to Host B^2 *via* a (Host B^1)–O21–H21 ··· O28–(Host B^2) interaction (d(O ··· O) = 2.833(3) Å).

These are two unique hydrogen bonds. Symmetry requirements generate another six hydrogen bonds, which interlink eight host molecules as shown in Fig. 5.

Because molecule A is on a centre of inversion, the 9,10-dihydroanthracene moiety of this molecule must be planar, but interestingly, in molecule B, which lies in a general position, the 9,10-dihydroanthracene moiety is bent away from planarity. In particular the centre ring displays a boat conformation. For a

† CCDC reference numbers 175482–175490. See http://www.rsc.org/suppdata/p2/b1/b110987c/ for crystallographic files in .cif or other electronic format.

Table 1 Crystal data, experimental and refinement parameters for compounds **1**–**9**

	1	**2**	**3**	**4**	**5**	**6**	**7**	**8**	**9**
Molecular formula	$C_{34}H_{36}O_2$	$C_{34}H_{36}O_2$·4(C_3H_7NO)	$C_{34}H_{36}O_2$·3(C_3H_7NO)·1(C_2H_6OS)	$C_{34}H_{36}O_2$·2(C_3H_7NO)·2(C_2H_6OS)	$C_{34}H_{36}O_2$·(C_3H_7NO)·3(C_2H_6OS)	$C_{34}H_{36}O_2$·4(C_2H_6OS)	$C_{34}H_{36}O_2$·4(C_3H_6O)	$C_{34}H_{36}O_2$·2(C_3H_7NO)·2(C_3H_6O)	$C_{34}H_{36}O_2$·2(C_2H_6OS)·2(C_3H_6O)
Host:guest ratio	—	1:4	1:3:1	1:2:2	1:1:3	1:4	1:4	1:2:2	1:2:2
M	476.63	769.01	774.04	779.08	784.11	789.14	708.94	738.98	749.04
Crystal symmetry	Monoclinic	Triclinic	Triclinic	Triclinic	Triclinic	Triclinic	Monoclinic	Triclinic	Triclinic
Space group	$P2_1/c$	$P\bar{1}$	$P\bar{1}$	$P\bar{1}$	$P\bar{1}$	$P\bar{1}$	$P2_1/c$	$P\bar{1}$	$P\bar{1}$
a/Å	16.6711(3)	9.0806(3)	9.0858(2)	9.1425(3)	9.0460(2)	9.0359(3)	8.9057(2)	8.9932(1)	8.9424(18)
b/Å	10.6712(2)	8.9414(4)	9.0547(2)	9.1730(3)	9.1291(2)	9.1353(3)	26.9049(6)	9.1674(1)	9.1788(18)
c/Å	24.3875(5)	14.935(1)	14.7684(4)	14.273(1)	14.409(1)	14.4126(6)	9.1615(2)	14.3817(2)	14.345(3)
α/°	90.00	74.477(2)	107.144(1)	71.356(1)	72.559(1)	72.981(1)	90.00	108.326(1)	72.25(3)
β/°	101.435(1)	88.693(2)	91.527(1)	81.229(1)	80.132(1)	80.086(1)	108.590(1)	92.808(1)	79.80(3)
γ/°	90.00	110.189(3)	70.236(2)	69.938(1)	71.486(2)	71.631(2)	90.00	70.886(1)	71.09(3)
Z	6	1	1	1	1	1	2	1	1
V/Å^3	4252.43(14)	1087.67(9)	1089.00(4)	1064.13(9)	1072.64(8)	1075.44(7)	2080.62(8)	1061.57(2)	1056.9(4)
μ (Mo-Kα)/mm^{-1}	0.068	0.077	0.123	0.173	0.218	0.264	0.073	0.076	0.171
Temperature of data collection/K	173	173	173	173	173	173	173	173	173
Range scanned, *θ*/°	2.30–27.17	2.41–27.49	2.39–29.62	2.37–27.48	2.38–25.02	2.84–27.48	2.46–25.70	1.49–27.50	2.89–28.29
Index range	$21 \geq h \geq 0$, $13 \geq k \geq 0$, $30 \geq l \geq -31$	$11 \geq h \geq -11$, $11 \geq k \geq -10$, $19 \geq l \geq -19$	$12 \geq h \geq -12$, $11 \geq k \geq -12$, $20 \geq l \geq -20$	$11 \geq h \geq -8$, $10 \geq k \geq -11$, $15 \geq l \geq -18$	$10 \geq h \geq -10$, $10 \geq k \geq -10$, $14 \geq l \geq -17$	$11 \geq h \geq -11$, $11 \geq k \geq -11$, $18 > l > -15$	$10 \geq h \geq -10$, $32 \geq k \geq -30$, $10 \geq l \geq -11$	$9 \geq h \geq -11$, $11 \geq k \geq -11$, $18 \geq l \geq -18$	$11 \geq h \geq -11$, $11 \geq k \geq -12$, $19 \geq l \geq -19$
No. reflections collected	8950	6935	11040	5770	5799	6220	11359	7598	7063
No. unique reflections	8950 ($R_{int} = 0.0000$)	4771 ($R_{int} = 0.0167$)	5998 ($R_{int} = 0.0234$)	4625 ($R_{int} = 0.0145$)	3694 ($R_{int} = 0.0164$)	4370 ($R_{int} = 0.0184$)	3911 ($R_{int} = 0.0451$)	4651 ($R_{int} = 0.0160$)	4985 ($R_{int} = 0.0166$)
No. reflections with $I > 2\sigma I$	6522	3093	4369	3420	3060	3683	2328	3708	4006
Data/restraints/parameters	8950/12/489	4771/0/259	5998/0/285	4625/2/251	3694/20/257	4370/0/247	3911/0/267	4651/0/266	4985/0/237
Final *R* indices ($I > 2\sigma I$)	$R_1 = 0.0752$, $wR_2 = 0.1953$	$R_1 = 0.0583$, $wR_2 = 0.1497$	$R_1 = 0.1139$, $wR_2 = 0.3709$	$R_1 = 0.0638$, $wR_2 = 0.1656$	$R_1 = 0.0816$, $wR_2 = 0.2087$	$R_1 = 0.0893$, $wR_2 = 0.2546$	$R_1 = 0.0596$, $wR_2 = 0.1679$	$R_1 = 0.0828$, $wR_2 = 0.2396$	$R_1 = 0.0793$, $wR_2 = 0.2195$
R indices (all data)	$R_1 = 0.1049$, $wR_2 = 0.2214$	$R_1 = 0.0991$, $wR_2 = 0.1811$	$R_1 = 0.1401$, $wR_2 = 0.3977$	$R_1 = 0.0908$, $wR_2 = 0.1840$	$R_1 = 0.0961$, $wR_2 = 0.2228$	$R_1 = 0.1003$, $wR_2 = 0.2690$	$R_1 = 0.1126$, $wR_2 = 0.2069$	$R_1 = 0.1000$, $wR_2 = 0.2551$	$R_1 = 0.0935$, $wR_2 = 0.2332$
Largest diff peak and hole (e Å^{-3})	0.809; −0.570	0.269; −0.250	0.914; −0.859	0.827; −0.543	1.360; −0.734	0.750; −0.710	0.378; −0.215	0.678; −0.365	0.926; −0.450

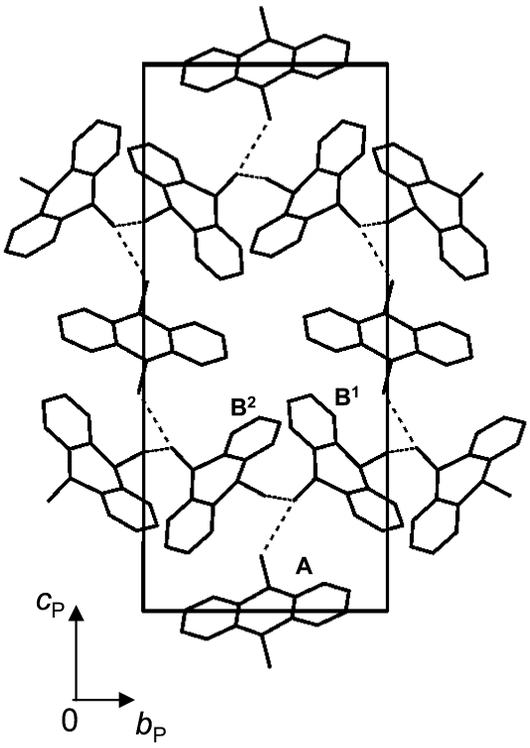

Fig. 5 Projection of the apohost structure along [100], showing the hydrogen bonding in the structure, with the *tert*-butylphenyl groups omitted for clarity, and with B^1 at (x,y,z) and B^2 at $(-x,y-1/2,1/2-z)$.

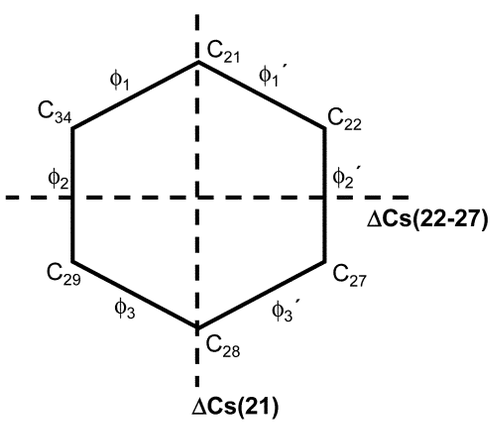

Fig. 6 Mirror plane asymmetry parameters calculated for the centre ring of the 9,10-dihydroanthracene moiety.

boat conformation, two mirror plane asymmetry parameters can be calculated. These are shown in Fig. 6. We have calculated the asymmetry parameters using eqns. (1) and (2),[11] and obtained values of $\Delta C_s(21) = 3.65$ and $\Delta C_s(22–27) = 3.96$. These values are small, which indicates that the ring deviates very little from the boat conformation.

$$\Delta C_s(21) = \sqrt{\frac{\sum_{i=1}^{3} (\phi_i + \phi_i')^2}{3}} \quad (1)$$

$$\Delta C_s(21-27) = \sqrt{\frac{(\phi_1 - \phi_3)^2 + (\phi_1' - \phi_3')^2}{2}} \quad (2)$$

Van der Waals plots of the surface showed that the hydroxyl groups protrude from the *ab* plane, so we surmise that this is the reactive face, which presents free OH donors for incoming acetone gas molecules for incipient host–guest hydrogen bonding. This is similar to the situation encountered with the structure of 1,1,6,6-tetraphenyl-hexa-2,4-diyne-1,6-diol, a host compound which also enclathrates acetone vapour.[12]

The structures of the A/B series, compounds **2**–**6**, are shown in Fig. 7a–7e. The five structures are all triclinic, space group $P\bar{1}$, with similar cell dimensions. In each case the host molecule is located at the origin on a centre of inversion, and the compounds are isostructural with respect to the host. The only differences are due to the locations of the guests, whose features are summarised in Table 2. In all cases only two guests are hydrogen bonded to the host. For the H·3A·B structure, symmetry requires the DMSO guest, B to be located at two sites, each with site occupancies of 0.5. The DMF molecules were refined with site occupancy factors of 0.75 each. These values were initially derived from difference electron density maps and were subsequently refined. The difference electron density map showed that the DMSO and DMF molecules share the same general location and we found their positions by contouring several layers of the difference electron density map and fitting models of the guest molecules to the peaks. The same procedure was followed for the compound H·A·3B.

In all the structures, the host molecules pack to form a series of continuous ribbons in the [001] direction, which are not interlinked. Within the host framework there are cavities containing the guest molecules. These cavities have a maximum cross section of 3.7 × 9.0 Å.

The structure of the inclusion compound with acetone, H·4C, is shown in Fig. 8. This structure is monoclinic and crystallises in the space group $P2_1/c$ with a host:guest ratio of 1:4. There are two host molecules per unit cell located at 0,1/2,0 and 0,0,1/2 (Wyckoff position c), while the guest molecules lie on general positions in the unit cell. Two of the guests are hydrogen bonded to the hydroxyl groups of the host molecule.

The packing of the host molecules results in criss-crossed channels running parallel to [100] and [001] in which the guest molecules are located. These channels meet at two locations in the unit cell: (0.2, 0.25, 0.5) and (0.8, 0.75, 0.5). The channels running parallel to [100] have a maximum cross section of 4.1 × 4.1 Å, while the channels running parallel to [001] have a maximum cross section of 5.3 × 8.4 Å.

The structures of inclusion compounds **8** and **9**, H·2A·2C and H·2B·2C respectively, are both triclinic and crystallise in the space group $P\bar{1}$. They have host:guest ratios of 1:4 and both have very similar cell dimensions and unit cell volumes to compounds **2**–**6**. They are also isostructural with compounds **2**–**6** with respect to the location of the host molecules. In both compounds, two guest molecules are hydrogen bonded to the host. In **8**, the two DMF guest molecules are hydrogen bonded, while in **9**, the DMSO molecules are hydrogen bonded to the host. In both cases, the acetone molecules are not hydrogen bonded. The DMF guest molecules in **8** and the acetone guest molecules in **9** are disordered.

Kinetics

The kinetics of enclathration between a solid organic host and vapour guest molecules has received little attention because such studies are experimentally difficult and the inclusion compounds formed are often unstable under ambient conditions. We have constructed an automated magnetic suspension balance for this purpose, which allows us to monitor the mass change of the inclusion compound with time under controlled conditions of pressure and temperature.[13]

The kinetic measurements were carried out by exposing finely powdered host compound to acetone vapour at fixed temperatures, but at various pressures of acetone, and recording the mass increase with time. Typical isothermal curves are shown in Fig. 9 for $T = 290$ K and vapour pressures varying from 86 to 158 Torr.

Table 2 Summary of hydrogen bonding in compounds **2**–**9**

Compound	Guest H-bonded *d*(O ··· O)/Å	Guest not H-bonded
2 H·4A	DMF O–H ··· O=C *d* = 2.728(2)	DMF Ordered
3 H·3A·1B	DMF O–H ··· O=C *d* = 2.622(4) DMSO O–H ··· O=S *d* = 2.880(6)	DMF Ordered, with a site occupancy factor of 0.75. DMF and DMSO share a common carbon atom (C29)
4 H·2A·2B	DMSO O–H ··· O=S *d* = 2.747(3)	DMF O atom disordered over 2 positions with site occupancy factors of 0.57 and 0.43
5 H·1A·3B	DMSO O–H ··· O=S *d* = 2.753(3)	DMF Ordered DMSO Molecule disordered over 3 positions with site occupancy factors of 0.25, 0.15 and 0.10, with 1 carbon on two of the molecules sharing a common atom site and a sulfur atom and an oxygen atom sharing a common atom site
6 H·4B	DMSO O–H ··· O=S *d* = 2.766(3)	DMSO Molecule disordered over 2 positions, with site occupancy factors of 0.58 and 0.42, with 1 carbon on each molecule sharing a common atom site
7 H·4C	Acetone O–H ··· O=C *d* = 2.855(2)	Acetone Ordered
8 H·2A·2C	DMF O–H ··· O=C *d*(O1 ··· O24) = 2.836(3) *d*(O1 ··· O29) = 2.662(8) Molecule disordered over 2 positions, with site occupancy factors of 0.67 and 0.33, but sharing a common nitrogen site	Acetone Ordered
9 H·2B·2C	DMSO O–H ··· O=S *d* = 2.766(3)	Acetone Severely disordered

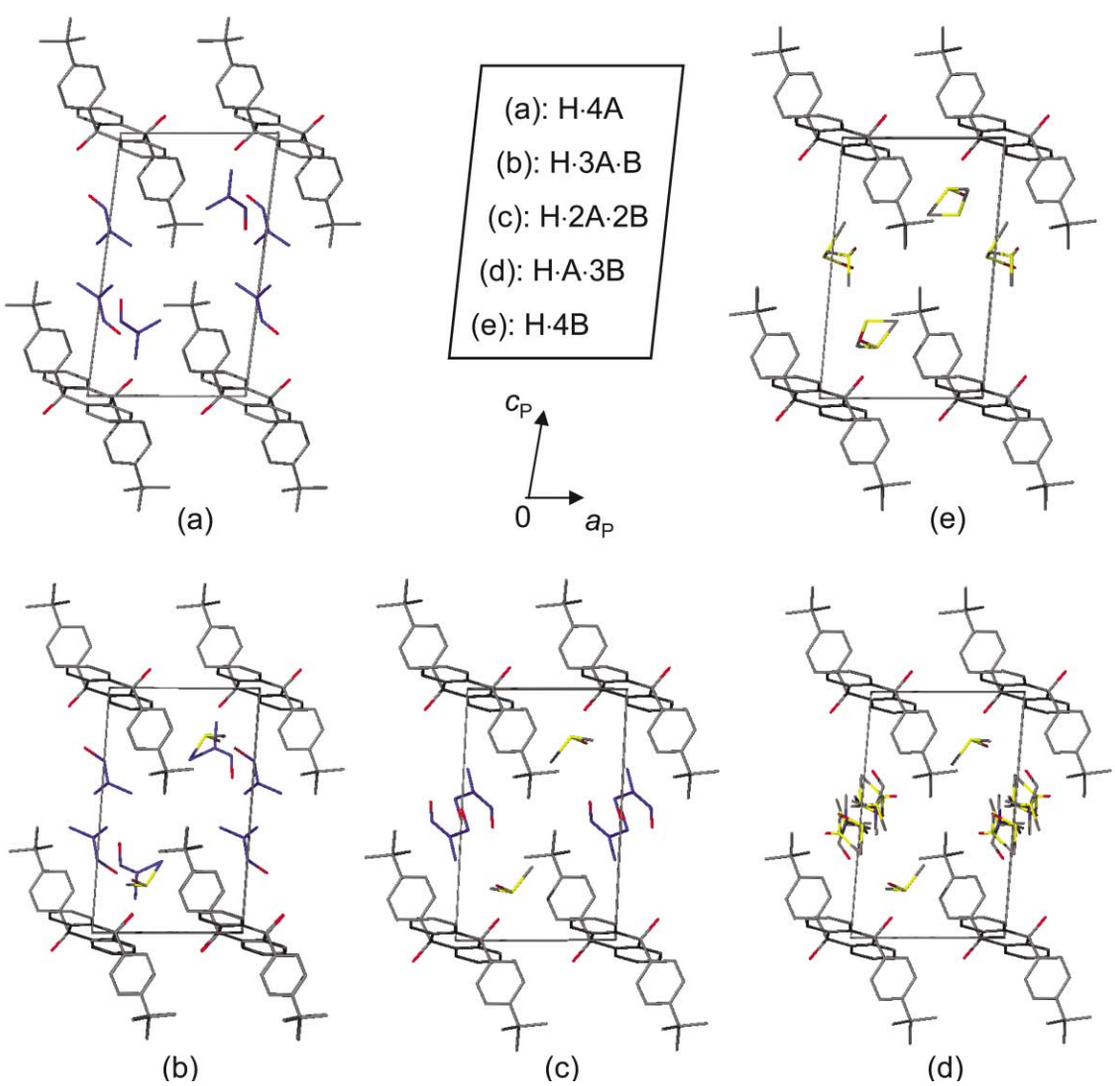

Fig. 7 Projection of the five structures of the A/B series along [010], with (a): H·4A, (b): H·3A·B, (c): H·2A·2B, (d): H·A·3B and (e): H·4B.

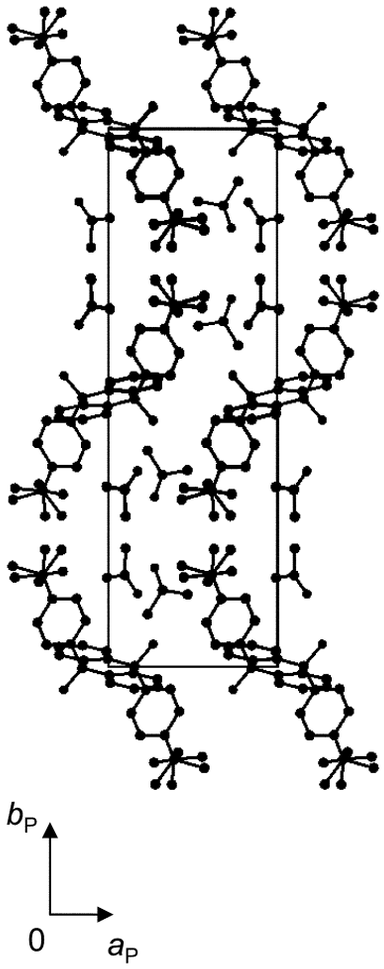

Fig. 8 Projection of the H·4C structure along [001].

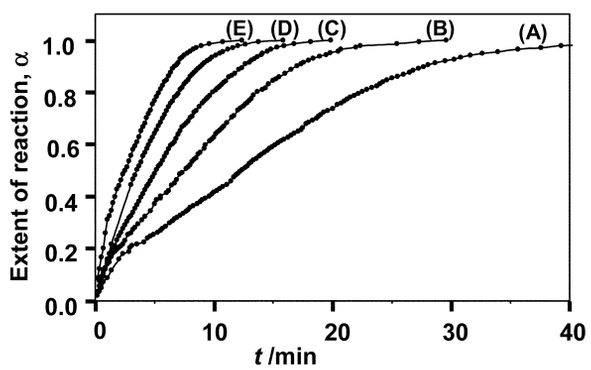

Fig. 9 Isothermal curves at T = 290 K, with vapour pressures of (A) 86 Torr, (B) 100 Torr, (C) 118 Torr, (D) 140 Torr, (E) 158 Torr.

We fitted the kinetic results to the contracting volume equation,[14] namely $f(\alpha) = 1 - (1 - \alpha)^{1/3}$, and derived the rate constants, k_{obs}. We noted that in order for the apohost to combine with acetone, a threshold pressure P_0 of the guest was required. We repeated these experiments at T = 298 K and 306 K. The plot of k_{obs} *vs.* the pressure of the guest, P, is shown in Fig. 10, which yielded the following P_0 values at the indicated temperatures: 62 Torr (290 K), 115 Torr (298 K), 127 Torr (306 K).

An interesting feature of the kinetics is that for a given pressure of acetone vapour, the rate of the reaction decreases with increasing temperature. This is clearly illustrated in Fig. 10, where for example, at a pressure of 140 Torr, k_{obs} is 0.061 min^{-1} at 290 K and 0.020 min^{-1} at 298 K. This anti-Arrhenius behaviour has been observed for enclathration of acetone

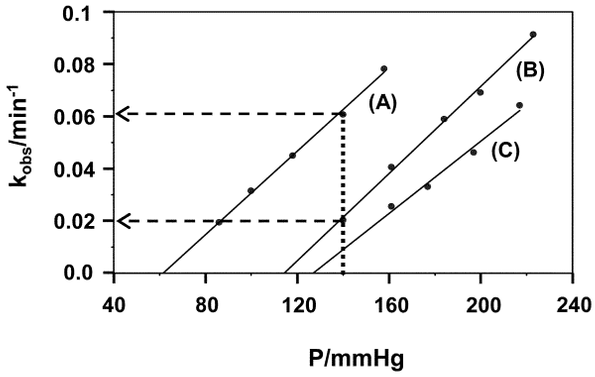

Fig. 10 Plot of k_{obs} *vs.* the pressure of the guest, P.

by the related host *trans*-9,10-dihydroxy-9,10-diphenyl-9,10-dihydroanthracene.[15]

This phenomenon arises from the threshold pressure, P_0, required to start the enclathration reaction. These threshold pressures increase with increasing temperatures, which is consistent with the inclusion compound having a greater propensity to decompose at higher temperatures. This threshold pressure phenomenon has also been observed in the absorption of ethyl acetate by anthracenebisresorcinol, which was monitored by pressure measurements, X-ray powder diffraction and thermal analysis.[16]

Using the same magnetic suspension apparatus, we studied the kinetics of desolvation by subjecting the system to vacuum at various temperatures. The desolvation curves were decelerator and the first order equation fitted over virtually the complete decomposition range (α = 0.05 to 0.95). The semilogarithmic plot of ln k_{obs} *vs.* 1000 K/T is shown in Fig. 11 and yielded an activation energy of 48.4 kJ mol^{-1}. Similar results were obtained for the desorption of acetone from the inclusion compound it forms with 2,2′-bis(2,7-dichloro-9-hydroxy-9-fluorenyl)-biphenyl.[17]

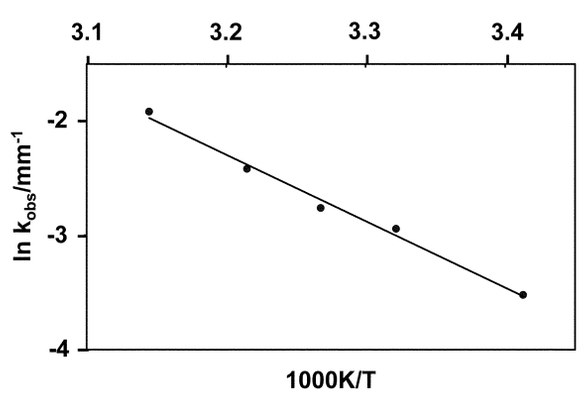

Fig. 11 Semilogarithmic plot of ln k_{obs} *vs.* 1000 K/T.

Conclusion

The field of inclusion compounds with mixed guests is an important one in which systematic studies may yet establish what aspects are important in the selection of different guests. These include steric factors, polarity, guest symmetry and solubility. In this regard it is noteworthy that the hexapedal host hexakis(3-hydroxy-3,3-diphenylprop-2-ynyl)benzene will form a stable mixed inclusion compound with benzene and acetonitrile, but not with either of the guests alone.[18]

The occurrence of ternary inclusion compounds in which the guest stoichiometry can be controlled has implications for crystal engineering.[19,20] This is significant in such fields as chemical sensors, optical and electronic properties of organic crystals as well as their thermal and kinetic properties.[21]

References

1 G. H. Gorbitz and H. P. Hersleth, *Acta Crystallogr., Sect. B*, 2000, **56**, 526.
2 R. E. Marsh, W. P. Schaefer, J. A. Hodge, M. E. Hughes, H. B. Gray, J. E. Lyous and P. E. Ellis Jr., *Acta Crystallogr., Sect. C*, 1993, **49**, 1339.
3 N. Hayashi, K. Karuma, Y. Mazaki, T. Imakubo and K. Kobayashi, *J. Am. Chem. Soc.*, 1998, **120**, 3799.
4 M. Kitamura, Y. Kawaguchi and F. Toda, *J. Incl. Phenom. Mol. Recognit. Chem.*, 1993, **15**, 27.
5 M. R. Caira, L. R. Nassimbeni, D. Vujovic and E. Weber, *J. Chem. Soc., Perkin Trans. 2*, 2001, 861.
6 A. M. Pivovar, K. T. Holman and M. D. Ward, *Chem. Mater.*, 2001, **13**, 3018.
7 M. R. Caira, A. Horne, L. R. Nassimbeni and F. Toda, *J. Mater. Chem.*, 1998, **8**, 1481.
8 E. de Vries, L. R. Nassimbeni and H. Su, *Eur. J. Org. Chem.*, 2001, 1887.
9 K. Dohi, K. Tanaka and F. Toda, *J. Chem. Soc. Jpn., Chem. Ind. Chem.*, 1986, 927.
10 M. R. Caira, T. le Roex and L. R. Nassimbeni, *Chem. Commun.*, 2001, 2128.
11 *Atlas of steroid structure*, ed. W. L. Duax and Dorita A. Norton, Plenum Data Company, New York, 1975, p. 18.
12 D. R. Bond, L. Johnson, L. R. Nassimbeni and F. Toda, *J. Solid State Chem.*, 1991, **92**, 68.
13 L. J. Barbour, K. Achleitner and J. R. Greene, *Thermochim. Acta*, 1992, **205**, 171.
14 A. K. Galwey and M. E. Brown, *Handbook of Thermal Analysis and Calorimetry*, ed. M. E. Brown, Elsevier Science B.V., Amsterdam, 1998, p. 162.
15 L. J. Barbour, M. R. Caira and L. R. Nassimbeni, *J. Chem. Soc., Perkin Trans. 2*, 1993, 2321.
16 T. Dewa, K. Eudo and Y. Aoyama, *J. Am. Chem. Soc.*, 1998, **120**, 8933.
17 M. R. Caira, A. Coetzee, L. R. Nassimbeni, E. Weber and A. Wierig, *J. Chem. Soc., Perkin Trans. 2*, 1997, 237.
18 S. A. Bourne, K. L. Gifford Nash and F. Toda, *J. Incl. Phenom. Mol. Recognit. Chem.*, 1998, **32**, 91.
19 G. R. Desiraju, *Crystal Engineering*, Elsevier, Amsterdam, 1989.
20 W. Jones, *Organic Molecular Solids*, CRC press, New York, 1997, ch. 6.
21 D. V. Soldatov and J. A. Ripmeester, *Chem. Eur. J.*, 2001, **7**, 2979.